STUDY ON THERMAL-MECHANICAL COUPLING OF THE CERAMIC LAYER IN DIESEL ENGINE PISTON WITH THERMAL BARRIER COATING

by

Xu LIN [*] ***and Yifei LI***

School of Civil and Transportation Engineering, Qinghai Minzu University, Xining, China

Original scientific paper
https://doi.org/10.2298/TSCI210705116L

Piston performance has an important on vehicle reliability, efficiency, and exhaust emissions. Application of the thermal barrier coating is an effective method for preventing heat transfer from combustion chamber to the substrate. The numerical model of thermal barrier coating piston is established by using finite element method, and a comprehensive thermal-mechanical result is given to determine the influence of ceramic thickness on ceramic layer and substrate. Compared with uncoated piston, the maximum temperature of substrate decreased by 3.34%, 4.09%, 5.19%, 5.95%, and 6.69%, corresponding to ceramic thicknesses of 0.15 mm, 0.2 mm, 0.25 mm, 0.3 mm, and 0.35 mm. The maximum thermal stress decreases from 78 MPa to 73 MPa. For ceramic layer of the thermal barrier coating piston, the maximum temperature appears at the top surface of the ceramic layer, while the maximum thermal stress occurs at the bottom of the ceramic layer. As the ceramics thickness increases from 0.15 mm to 0.35 mm, the maximum temperature of the ceramic layer increases from 322 ℃ to 377 ℃, while the maximum thermal stress decreases from 95 MPa to 89 MPa. Thermal-mechanical coupled stress analysis shows that the maximum coupling stress occurs at the pinhole and its value does not change significantly. The thickness of the ceramic layer has little effect on the pinhole, but has a great influence on the ceramic layer.

Key words*: piston, ceramic layer, thermal barrier coating, numerical simulation, temperature field, thermal stress, thermal-mechanical coupling stress*

Introduction

As one of the key components of Diesel engine, the piston works in a hostile environment withstanding cyclic high-strength mechanical loads and extreme temperatures. The combustion chamber of the piston is directly in touch with high-temperature gas during the working process [1-3]. Traditionally, the heat of the piston is dissipated through the cooling system. Further, the metallic components of the piston have the property of high thermal conductivity. The heat loss of the engine is large and the thermal efficiency needs to be improved [4, 5].

In recent years, thermal barrier coating (TBC) has been widely used in the aerospace and automotive industries because of their advantageous characteristics such as high melting

[*]Corresponding author, e-mail: linxuaaa@126.com

point, low density, low thermal conductivity, erosion and oxidation resistance. The TBC is applied in Diesel engine for thermal fatigue protection of substrate and reduced in heat transfer from combustion chamber to substrate, also for possible decrease of fuel consumption and avoidance of corrosion caused by contaminants [6-9].

The insulation of the ceramic layer affects the heat conduction and, hence, improves the thermal physical properties and reduces the heat loss of the Diesel engines [10-13]. Moreover, the expectation of improving the thermal efficiency of the piston can bring the application of higher compression ratios, and can reduce in-cylinder heat rejection. On the other hand, thermophysical properties of the TBC and their difference of materials in each layer, have an important impact on the ceramic layer or piston through the effect of load distribution and thermal mismatch [14, 15]. These factors cause redistributed temperature field, thermal and thermal-mechanical stresses of TBC piston. In order to meet the technical requirements in the manufacturing process, it is important to predict the temperature field, thermal and thermal-mechanical stresses of the TBC piston.

Buyukkaya [16] used MgO-ZrO_2 material as coating and studied the temperature field of coated piston by finite element method. From the analysis, it was concluded that the maximum temperature of the TBC piston increased 48% for the aluminum silicon alloy and 35% for the steel compared with uncoated piston. Cerit and Coban [17] investigated the thermal behavior of spark ignition engine piston for various thickness of ceramic layer. From the analysis, it was concluded that the normal stress decreased with coating thickness, which was a function of ceramic thickness. Gehlot and Tripathi [18] studied the temperature field of Diesel engine piston. The results showed that with the increase of the thickness of ceramic layer, the temperature of the top surface increased and the temperature of the substrate decreased. Numerical investigation of the 1.6l automotive Diesel engine was carried out by Garud *et al.* [19]. The results found that the fuel consumption and heat transfer reduction of the TBC piston was found 1% and 6% lower, respectively, compared to uncoated piston. Similar conclusion has been reached by Broatch *et al.* [20]. He concluded that compared with uncoated engine, the heat loss of coated engine is reduced by 5%, however, the knock tendency increased. Reghu *et al.* [21] studied the effect of coating on Si-Al alloy substrate by spraying a coating on the surface of the Si-Al alloy. He showed that the coating could reduce the heat loss of the piston and could improve the temperature of the combustion chamber. He also got the same conclusion by numerical simulation based on ANSYS.

The coating thickness has a strong influence on the temperature and stress of TBC piston. The ceramic layer is a key component in protecting the substrate due to low thermal conductivity. On the other hand, the detachment of ceramic layer from adhesive layer is responsible for a limited life. It is necessary to investigate the temperature and thermal-mechanical stresses distribution of the ceramic layer separated from the piston. It is also important to study the thermal and thermal-mechanical stresses of the TBC piston in order to control the thermal and thermal-mechanical stresses within acceptable values. The simulation of thermodynamic calculation can effectively save time and reduce cost in manufacturing of TBC piston. In this paper, a Diesel engine piston with 85 mm cylinder diameter is studied. The main emphasis of this paper is to investigate thermal and thermal-mechanical behavior of the ceramic layer and substrate by using various thicknesses of the ceramic layer.

Materials and methods

Finite element model

The piston is made of aluminum alloy. Mechanical properties of the piston are 490 MPa, 470 MPa, and 305 MPa for ultimate, yield and shear strength, respectively. The TBC is

located at the surface of the TBC piston and composed of adhesive layer and ceramic layer. The thermal insulation ceramic layer is zirconia based material. The adhesive layer is NiCrAl metal material. The adhesive layer ensures the adhesion between the ceramic layer and the metal substrate, and has similar physical properties to the piston under the premise of considering the compatibility. Assuming that each layer is uniform, the elastic modulus, poisson's ratio and other parameters of each part in 20 ℃ and 800 ℃ are reported in tab. 1 [22-24].

Table 1. Physical properties of materials for TBC piston

Component	Elastic modulus [Gpa]		Poisson's ratio		Thermal conductivity [$Wm^{-1}°C^{-1}$]		Thermal expansion [$\times10^{-6}$ $°C^{-1}$]	
	20 ℃	800 ℃	20 ℃	800 ℃	20 ℃	800 ℃	20 ℃	800 ℃
Ceramic layer	46	35	0.2	0.22	1.2	1.25	8	12
Adhesive layer	105	95	0.27	0.29	16	21	12	17
Piston	130	115	0.3	0.33	130	139	20	31

To reduce the number of elements and save solving time, small parts such as pins and chamfering that do not affect the whole piston are ignored. The piston model is meshed by thermal-mechanical coupling elements with eight nodes. To improve the accuracy of simulation, the mesh of the ceramic layer and the adhesive layer is refined to ensure the uniformity of each layer and the smoothness of grid connection between layers. The thickness of the adhesive layer is defined as 0.1 mm, and the thickness of ceramic layer has been changed from 0.15 mm to 0.35 mm with a 0.05 mm increment. When the thickness of adhesive layer and ceramic layer are 0.1 mm and 0.15 mm, respectively, the finite element model of the TBC piston is shown in fig. 1. The finite element model consists of 360505 nodes and 229028 elements, including 21724 nodes and 10230 elements in the adhesive layer, 23886 nodes, and 11841 elements in the ceramic layer.

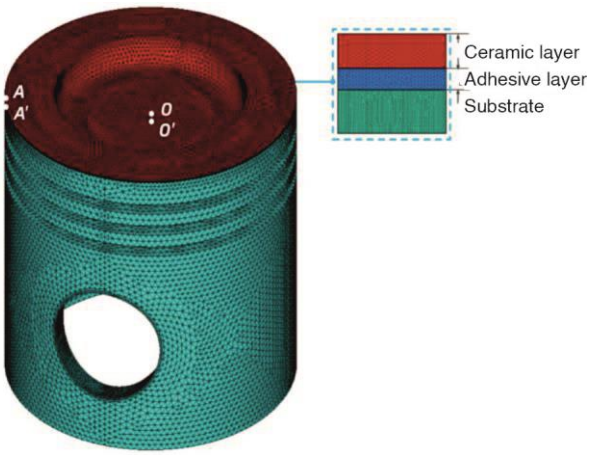

Figure 1. Finite element model of the TBC piston

Thermo-mechanical boundary conditions

The piston temperature field is defined as a steady-state condition that is related to the space position but not with time. The correct thermal boundary condition is the key to investigate the thermal and thermo-mechanical behavior of the TBC piston. The piston has an irregular structure. It is difficult to measure the temperature of the piston. The accuracy of the results cannot be guaranteed by obtaining the first and second boundary conditions of the piston by experimental methods. The third boundary condition is adopted, which is to determine the average temperature of the working environment and the convective heat transfer coefficient of the piston. The thermal boundary conditions of the TBC piston are adapted from [25-27], as shown in tab. 2.

Table 2. Average temperature and heat transfer coefficient of TBC piston

Boundary area		Ambient temperature [°C]	Heat transfer coefficient [$Wm^{-2}K^{-1}$]
Combustion chamber		800	620
Combustion chamber edge		800	670
Firepower bank		220	280
First ring	Upper and lower edge	180	1584
	Bottom surface		982
	Ring land		587
Second ring	Upper and lower edge	180	1325
	Bottom surface	180	982
	Ring land	180	587
Third ring	Upper and lower edge	160	1172
	Bottom surface	160	982
	Ring land	170	587
Skirt		100	425
Piston cavity	Inner top surface	100	717
	Inner middle surface	100	635
	Inner bottom surface	100	529
Pin hole		90	261

The rated speed of the Diesel engine is 3200 rpm. From the piston indicator diagram, the maximum combustion pressure in the combustion chamber is 12.5 MPa. The mechanical load of the TBC piston mainly includes the gas pressure, the reciprocating inertia force in the cylinder liner, and the lateral thrust due to the swing of the connecting rod. The combustion gas pressure is applied on the combustion chamber and firepower bank. The reciprocating inertia force of piston is loaded by acceleration.

Results and discussion

Temperature field analysis

To understand the effect of the ceramic layer, uncoated piston and TBC piston in different ceramic layer were analyzed. The thickness of ceramic layer analyzed were: 0.15 mm, 0.20 mm, 0.25 mm, 0.30 mm, and 0.35 mm. The temperature distribution of uncoated piston and TBC piston with different ceramics thickness from 0.15 mm to 0.35 mm in sequence are shown in fig. 2(a)-2(f). It was observed that the treads of temperature distribution of the uncoated and TBC piston are similar. The highest temperature are localized in the combustion chamber and, in particular, around the edge of combustion chamber. Since combustion chamber is directly in touch with gas, the temperature of combustion chamber is extremely high. The temperature of the substrate significantly dropped from the head to skirt along the axis. The maximum temperature of uncoated piston is 269 °C. For TBC piston with different thickness from 0.15 mm to 0.35 mm, the maximum temperature are 322 °C, 336 °C, 351 °C, 365 °C, and 377 °C, respectively. Compared to the uncoated piston, the temperature of the fire bank and piston ring of the TBC piston is significantly lower. The difference of the skirt is not significant. The minimum temperature of both uncoated and coated pistons is about 96 °C.

Compared to the results in reference [18, 28], the difference in the temperature values of the piston is due to the difference in piston geometry and thermal boundary conditions, as well as the slight difference in the characteristics of the coating material used. However, the overall distribution of the temperature field is consistent, which proves the effectiveness of the method.

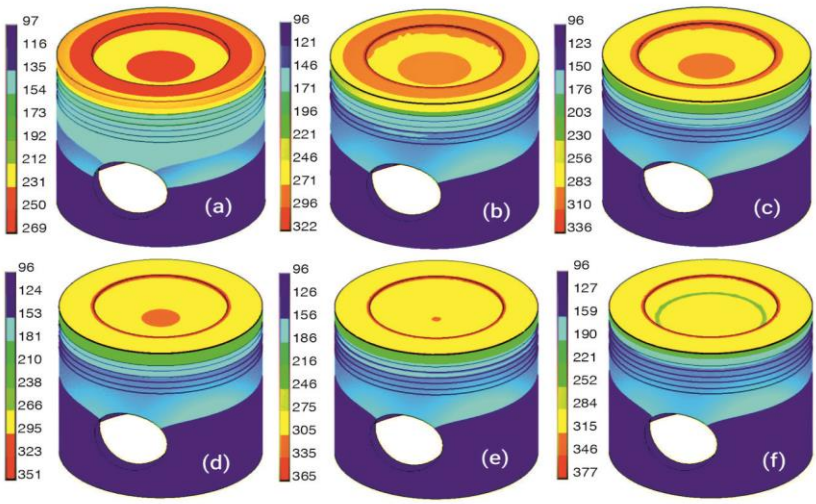

Figure 2. Temperature distribution of uncoated and TBC pistons

Cloud images of the temperature distribution of the ceramic layer for the TBC piston with different ceramics thickness from 0.15 mm to 0.35 mm in sequence are shown in fig. 3(a)-3(e). It is observed that the cloud images of the ceramic layer are similar to each other. As the thickness of ceramic layer increases, the maximum temperature of the ceramic layer increased from 322 °C to 377 °C and the minimum temperature dropped from 233 °C to 225 °C. Figure 4 illustrates that the difference of the ceramic layer are 89 °C, 105 °C, 122 °C, 138 °C, and 152 °C, respectively, corresponding to ceramic thicknesses of 0.15 mm, 0.2 mm, 0.25 mm , 0.3 mm, and 0.35 mm. The low thermal conductivity of ceramic layer is responsible for this kind of law. Ceramic layer can prevent heat transfer from upper surface to lower surface. The temperature drops sharply as it passes through the ceramic layer. The TBC can effectively prevent heat loss and improve the temperature at the top of TBC piston. The temperature variation law of TBC piston is consistent with the actual working condition.

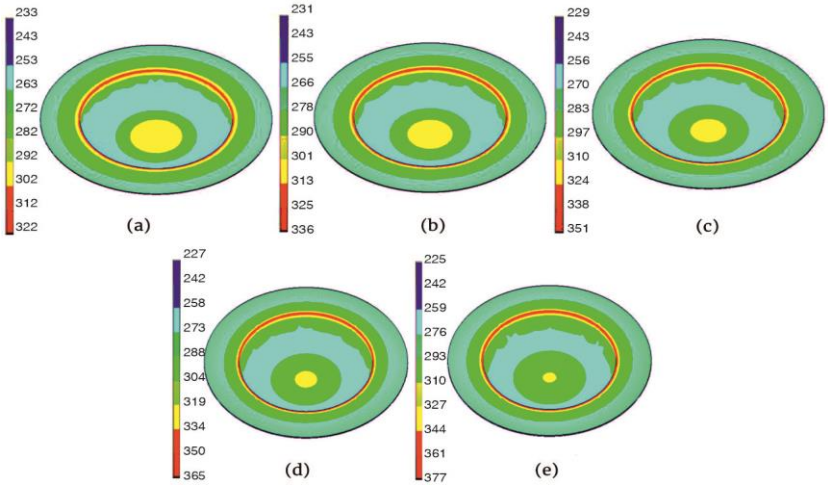

Figure 3. Temperature distribution of ceramic layer with different ceramics thickness

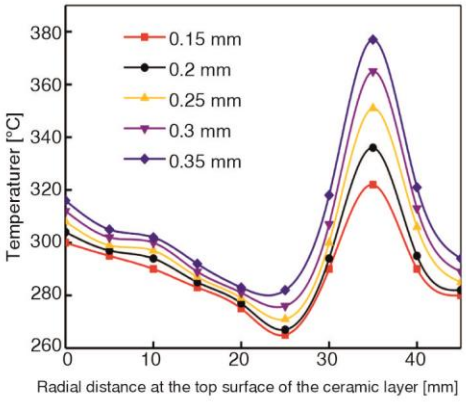

Figure 4. Temperature at the top surface of ceramic layer

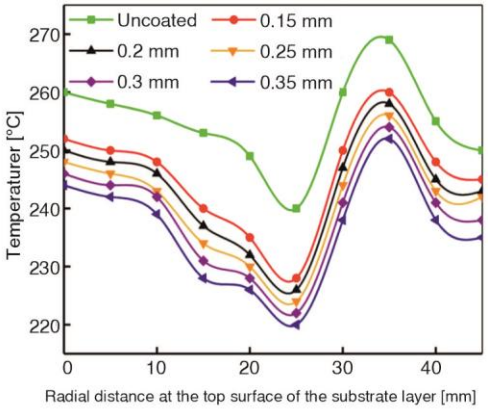

Figure 5. Temperature at the top surface of substrate

To understand the influence of the ceramics thickness on the temperature distribution, two paths called radial distance are defined along the line OA and line O'A', respectively, (see fig. 1). The O'A' starts from the center O' of the top surface of the substrate and ends at the outer edge A' of the substrate. The OA starts from the center O of the ceramic coating and ends at the outer edge A of the ceramic layer. Temperature distributions versus radial distance for ceramic layer in different ceramics thickness is plotted in fig. 4. At the top surface of the ceramic coat, the temperature gradually decreases from the center to the edge of the bowl and changes its direction. The temperature reaches its maximum at the throat and sharply decreases from the throat to the edge along the radial direction. As expected, the temperature at the top of ceramic layer increases with the increase of the thickness of the ceramic layer. Temperatures at the top surface of ceramic layer for various thicknesses along the line OA are roughly parallel to each other. The temperature increase on the top surface provides a beneficial factor to the utilization rate and the thermal efficiency of the TBC piston. Temperature distribution *vs.* radial distance for substrate in different ceramics thickness is plotted in fig. 5. Figure 5 includes uncoated pistons. For TBC piston, the temperature on the top surface of the substrate is obviously lower than that of uncoated piston due to the thermal insulation properties of the ceramic coating. Compared to the uncoated piston, the maximum temperature of the substrate decreases by 3.34%, 4.09%, 5.19%, 5.95%, and 6.69% for ceramic layer with a thickness of 0.15 mm, 0.2 mm, 0.25 mm, 0.3 mm, and 0.35 mm, respectively. The heat transferred from the combustion chamber to the substrate decreases with the increase of the thickness of the ceramic coating. As everyone knows, the strength of the piston increases with the lower temperature. As a result, the temperature reduction on the substrate is beneficial to increase piston life.

Thermal stress analysis

The temperature elements is converted into structural calculation elements. The results of temperature field calculation are applied to study the thermal stress of the uncoated and TBC piston.

For a 0.15 mm of thickness of ceramic layer, the thermal stress of substrate and ceramic layer are shown in figs. 6(a) and 6(b). The values of maximum thermal stress for substrate and ceramic layer are obtained 78 MPa and 95 MPa respectively. As expected, the max-

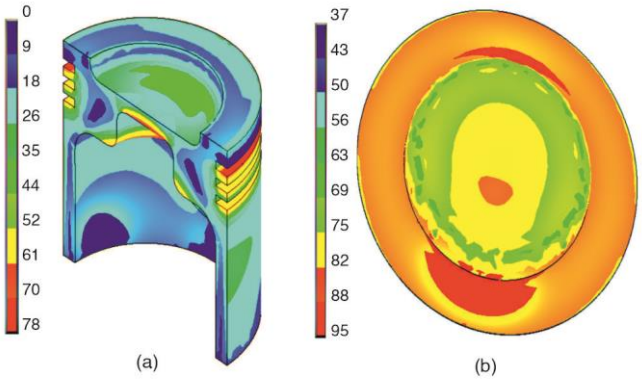

Figure 6. Thermal stress [MPa] of the TBC piston with a 0.15 mm ceramic thickness

imum thermal stress of substrate is observed at first ring groove. As is known to all, the heat flux density of the first ring groove reaches the maximum value, resulting in large heat transfer and exchange. Moreover, according to fig. 2, the temperature values of the upper part and the lower part of the first ring groove are obviously different, which leads to the significant thermal expansion of the material. As a result, the maximum stress value will be appear at the first ring groove. The thermal stress of the skirt is lower than 26 MPa, which can be ascribed to the lower temperature and smaller temperature gradient of the skirt.

As shown in fig. 6(b), the maximum thermal stress of ceramic layer is observed at the lower surface of ceramic layer, that is, the interface between the ceramic coating and the adhesive coating. According to fig. 3, the main reason for this phenomenon is that the temperature of the ceramic layer varies greatly. In addition, The upper surface of the ceramic layer expands freely under the action of heat load. On the contrary, the lower surface of the ceramic layer is constrained by adjacent geometry and is subjected to extrusion.

Under the same conditions, the uncoated piston is studied and its contour plots of thermal stress is shown in fig. 7. Compared with fig. 6(a), the contour plots of the uncoated piston is similar to that of the substrate of TBC piston. The maximum thermal stress of uncoated piston is 6 MPa higher than that of substrate with a 0.15 mm ceramic thickness, since The ceramic layer effectively blocks the heat transfer from the top surface to substrate for the TBC piston. Thanks to the TBC, the maximum thermal stress of the coated piston occurs at

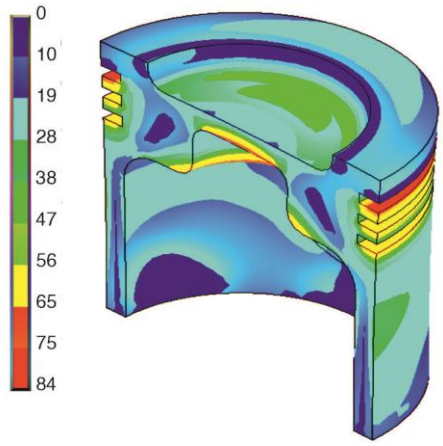

Figure 7. Thermal stress [MPa] of the uncoated piston

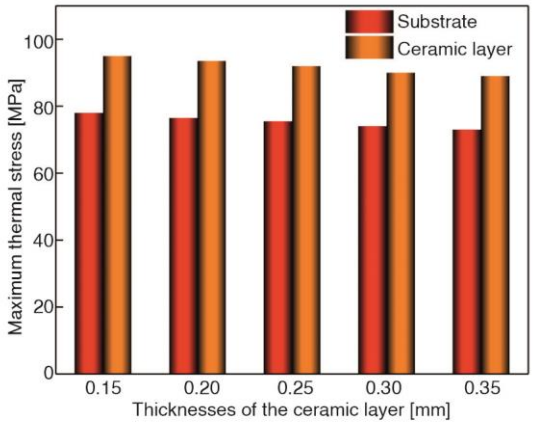

Figure 8. Thermal stress [MPa] of substrate and ceramic layer for TBC pistons

the bottom of the ceramic layer, while the thermal stress of the uncoated piston occurs at the first ring groove. The maximum thermal stress of ceramic layer of TBC piston is significantly higher than that of uncoated piston. Figure 8 shows the variation of the maximum thermal stress for substrate and ceramic layer in different ceramics thickness. Because of the lower thermal conductivity of ceramic coating, the maximum thermal stress of the substrate and ceramic layer are diminished with the increase of thickness of ceramic coating. As the thickness increases from 0.15 mm to 0.35 mm, the maximum thermal stress of substrate decreases from 78 MPa to 73 Mpa, and the maximum thermal stress of ceramic layer decreases from 95 MPa to 89 MPa. Combined with fig. 7, this result is consistent with the above analysis of the piston temperature field. The TBC can not only increase the temperature of the combustion chamber, but also block the heat transfer to the substrate. It can protect the substrate from heat damage.

Thermal-mechanical coupling stress analysis

In order to simulate the working condition of piston comprehensively, mechanical load is applied to piston based on thermal stress analysis. Figure 9(a) and 9(b) show the thermal-mechanical coupling stress of substrate and ceramic layer for 0.15 mm ceramics thickness. The maximum coupling stress value of substrate is determined 269 MPa at the upper part of the pinhole. Compared with the thermal stress analysis of the substrate, the move of the maximum stress from the first ring groove to the pin seat of the piston has been attributed to the pinhole is subjected to the combined action of mechanical load and thermal load. Since the pinhole contacts with the connecting rod and its structure has a narrow and round tip, the coupling stress has been observed at the seat of piston pin rather than the first ring groove.The maximum coupling stress value of ceramic layer is determined 120 MPa at the lower surface of ceramic layer. The coupling stress of ceramic layer is a complex stress coupling rather than the algebraic sum of thermal stress and mechanical stress. The ceramic layer is expanded under thermal stress and compressed under mechanical load. The deformation of ceramic layer caused by thermal stress is offset by the deformation caused by mechanical load. As a result, the coupling stress distribution at the lower surface of the ceramic layer is more uniform than the thermal stress distribution.

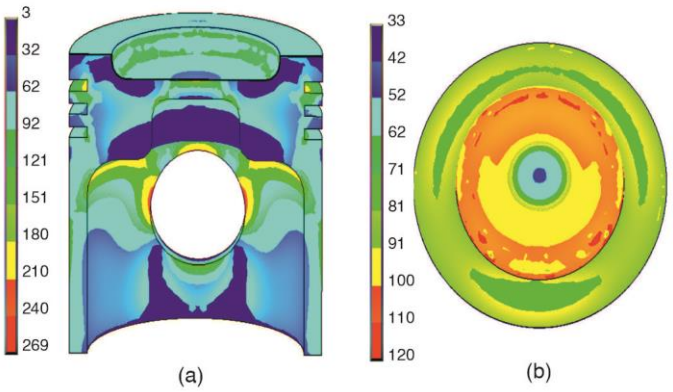

Figure 9. Thermal-mechanical coupling stress [MPa] of the TBC piston with a 0.15 mm ceramic thickness

The thermal-mechanical coupling stress of the uncoated piston is shown in fig. 10. Compared with TBC piston for 0.15 mm coating thickness, at the same location on the piston, in particular, around the pinhole of the piston, the treads of coupling stress distribution are similar. There is no significant difference in the maximum coupling stress between uncoated piston and TBC piston. Coupling stress at the combustion center for uncoated piston is much higher than substrate of the TBC piston. Compared with the thermal load, the mechanical load

has effect on stress of piston pinhole. Figure. 11 shows the variation of the maximum thermal-mechanical coupling stress for substrate and ceramic layer in different ceramics thickness. For the substrate and the ceramic layer only the value changes and the law of stress nephogram remain the same. From the fig. 11, it was observed that the maximum thermal-mechanical stress values at the pinhole is in the rage of 265-269 MPa. It does not change significantly, since the thermal stress changes little and the mechanical load remains constant for various thickness values. Due to the influence of thermal stress, the maximum coupling stress value of ceramic layer decreases gradually in various ceramics thickness. As the ceramics thickness increased from 0.15 mm to 0.35 mm, the maximum coupling stress of the ceramic layer decreased from 120 MPa to 110 MPa. Compared with the fig. 8, the thermal stress has more influence on the ceramic layer. Depending on the characteristic of the brittleness, any small defect on the ceramic layer has the potential of crack propagation under the cyclic thermal stress. In addition, the maximum coupling stress of the ceramic layer occurs at the lower surface of ceramic layer. As a result, it is extremely important to study clearly the thermal- mechanical stress distribution and ensure the machining accuracy of ceramic coating.

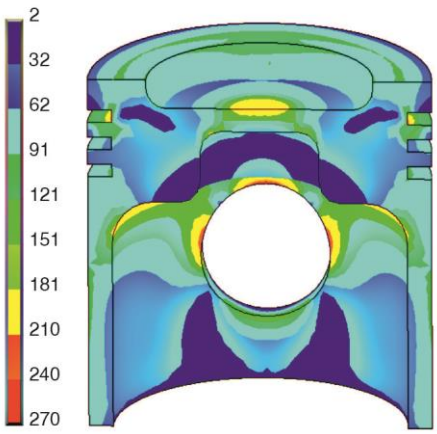

Figure 10. Thermal-mechanical coupling stress [MPa] of the uncoated piston

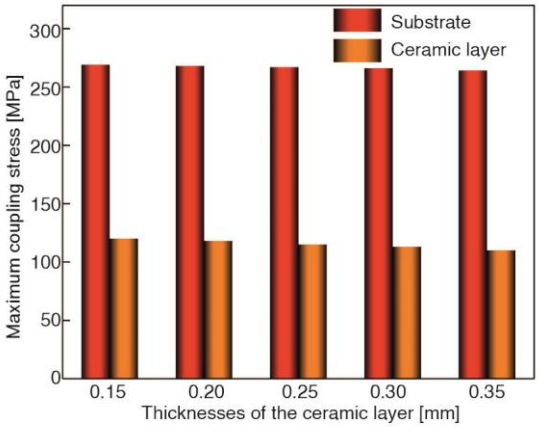

Figure 11. Thermal-mechanical coupling stress [MPa] of the substrate and the ceramic layer for TBC

Conclusions

The finite element model of the TBC piston is established and calculated. Firstly, the temperature field of the coated piston model with different ceramic thickness is evaluated, and then the thermal load and mechanical load are considered to better understand the effect of ceramic layer thickness on the piston. Temperature field shows that the TBC can increase the temperature of the combustion chamber and reduce the thermal energy transferred from the combustion chamber to substrate. The maximum temperature of the substrate decreases and the maximum temperature of the ceramic layer decreases with the ceramics thickness. Increasing the thickness of the ceramic layer can significantly reduce the heat loss of the TBC piston and protect the substrate from heat damage.

The numerical simulation of the thermal stress indicates that the maximum thermal stress of uncoated piston occurs at the first ring, while the maximum thermal stress of coated piston appears at the interface between ceramic layer and adhesive layer. For TBC piston, the

maximum thermal stress of the substrate and ceramic layer decreases with the increase of ceramics thickness. Compared with uncoated piston, the application of TBC can improve the thermal load carrying capacity. However, the overall thermal stress of the TBC piston simultaneously increases. The TBC may fail due to the ceramic layer falling off from the adhesive layer. Thermal-structure coupling analysis shows that the maximum coupling stress of the uncoated and TBC piston occurs at the pinhole and its value has not changed significantly. The maximum coupling stress of the ceramic layer occurs at the interface between the ceramic coat and the adhesive layer. The maximum thermal-structure coupling stress of substrate is mainly affected by the mechanical load, while the thermal-structure coupling stress of ceramic layer is dominated by the thermal stress.

In future research, a more detailed grid should be established to improve the accuracy of the coupling analysis of the coating interface and piston. Transient analysis can be calculated to evaluate the stress state of the piston during cyclic operation. Moreover, the fatigue life of the TBC piston should be further predicted, which provides a more perfect theoretical basis for the design of ceramic coating piston.

Acknowledgment

The authors gratefully acknowledge support by the 2022 Basic Research Program of Qinghai Province (No. 2022-ZJ-757).

References

[1] Silva, F. S., Fatigue on Engine Pistons – A Compendium of Case Studies, *Engineering Failure Analysis, 13* (2006), 3, pp. 480-492
[2] Guan, Z., Cui, Y., Thermal Load Analysis and Control of Four-Stroke High Speed Diesel Engine, *Thermal Science, 25* (2021), 4a, pp. 2665-2675
[3] Szmytka, F., *et al*., Thermal Fatigue Analysis of Automotive Diesel Piston: Experimental Procedure and Numerical Protocol, *International Journal of Fatigue, 73* (2015), Apr., pp. 48-57
[4] Floweday, G., *et al*., Thermo-Mechanical Fatigue Damage and Failure of Modern High Performance Diesel Pistons, *Engineering Failure Analysis, 18* (2011), 7, pp. 1664-1674
[5] Abedin, M. J., *et al*., An Overview on Comparative Engine Performance and Emission Characteristics of Different Techniques Involved in Diesel Engine as Dual-Fuel Engine Operation, *Renewable & Sustainable Energy Reviews, 60* (2016), July, pp. 306-316
[6] Wud, G., *et al*., Thermal Barrier Coatings with Novel Architectures for Diesel Engine Applications, *Surface and Coatings Technology, 396* (2020), 125950
[7] Wud, G., *et al*., Suspension Plasma-Sprayed Thermal Barrier Coatings for Light-Duty Diesel Engines, *Journal of Thermal Spray Technology, 28* (2019), 2, pp. 1674-1687
[8] Thibblin, A., *et al*., Influence of Microstructure on Thermal Cycling lifetime and Thermal Insulation Properties of Yttria-Stabilized Zirconia Thermal Barrier Coatings for Diesel Engine Applications, *Surface and Coatings Technology, 350* (2017), Sept., pp. 1-11
[9] Caputo, S., *et al*., Numerical and Experimental Investigation of a Piston Thermal Barrier Coating for an Automotive Diesel Engine Application, *Applied Thermal Engineering, 162* (2019), 114233
[10] Sivakumar, G., Investigation on Effect of Yttria Stabilized Zirconia Coated Piston Crown on Performance and Emission Characteristics of a Diesel Engine, *Alexandria Engineering Journal, 53* (2014), 4, pp. 787-794
[11] Padture, N. P., Advanced Structural Ceramics in Aerospace Propulsion, *Nature Materials, 15* (2016), 8, p. 804
[12] Clarke, D. R., *et al*., Thermal Barrier Coatings for More Efficient Gas-Turbine Engines, *MRS Bulletin, 37* (2012), 10, pp. 891-899
[13] Ozel, S., *et al*., Optimization of the Effect of Thermal Barrier Coating (TBC) on Diesel Engine Performance by Taguchi Method, *Fuel, 263* (2020), 116537
[14] Gupta, M., *et al*., Improving the Lifetime of Suspension Plasma Sprayed Thermal Barrier Coatings, *Surface and Coatings Technology, 332* (2017), Dec., pp. 550-559

[15] Che, C., *et al*., Uneven Growth of Thermally Grown Oxide and Stress Distribution in Plasma-Sprayed Thermal Barrier Coatings, *Surface and Coatings Technology, 203* (2009), 20-21, pp. 3088-3091
[16] Buyukkaya, E, Thermal Analysis of Functionally Graded Coating Alsi Alloy and Steel Pistons, *Surface and Coatings Technology, 202* (2008), 16, pp. 3856-3865
[17] Cerit, M., Coban, M., Temperature and Thermal Stress Analyses of a Ceramic-Coated Aluminum Alloy Piston Used in a Diesel Engine, *International Journal of Thermal Sciences, 77* (2014), 1, pp. 11-18
[18] Gehlot, R., Tripathi, B., Thermal Analysis of Holes Created on Ceramic Coating for Diesel Engine Piston, *Case Studies in Thermal Engineering, 8* (2016), Sept., pp. 291-299
[19] Garud, V., *et al*., Performance and Combustion Characteristics of Thermal Barrier Coated (YSZ) Low Heat Rejection Diesel Engine, *Mater. Today: Proc, 4* (2017), 2A, pp. 188-194
[20] Broatch, A., *et al*., Numerical Simulations for Evaluating the Impact of Advanced Insulation Coatings on H2 Additivated Gasoline Lean Combustion in a Turbocharged Spark-Ignited Engine, *Applied Thermal Engineering, 148* (2019), Feb., pp. 674-683
[21] Reghu, V. R., *et al*., Investigation on Thermal Barrier Effects of 8YPSZ Coatings on Al-Si Alloy and Validation Through Simulation, *Materials Today: Proceedings, 19* (2019), Part 2, pp. 630-636
[22] Dhomne, S., Mahalle, A. M, Thermal Barrier Coating Materials for SI Engine, *Journal of Materials Research and Technology, 8* (2019), 1, pp. 1532-1537
[23] Wang, H., *et al*., Development of a Thermal Transport Database for Air Plasma Sprayed ZrO_2-Y_2O_3 Thermal Barrier Coatings, *Journal of Thermal Spray Technology, 19* (2010), 5, pp. 879-883
[24] Qi, H. Y., *et al*., In-Situ Measurement of Elastic Modulus for Ceramic Top-Coat at High Temperature, *Journal of Central South University of Technology (English Edition), 15* (2008), Apr., pp. 372-376
[25] Zhang, H., *et al*., Thermal Analysis of Diesel Engine Piston, *Journal of Chemical & Pharmaceutical Research, 5* (2013), 9, pp. 388-393
[26] Adrian, I., Convective Heat Transfer Equation for Turbulent Flow in Tubes Applied to Internal Combustion Engines Operated Under Motored Conditions, *Applied Thermal Eng., 50* (2013), 1, pp. 536-545
[27] Liu, X. F., *et al*., Finite Element Analysis of Thermo-Mechanical Conditions Inside the Piston of a Diesel Engine, *Applied Thermal Engineering, 119* (2017), June, pp. 312-318
[28] Yao, Z. M., Li, W. G., Microstructure and Thermal Analysis of APS Nano PYSZ Coated Aluminum Alloy Piston, *Journal of Alloys and Compounds, 812* (2020), 152162

Paper submitted: July 5, 2021
Paper revised: July 1, 2022
Paper accepted: July 12, 2022